Supplementary Information

Highly Reversible Potassium-ion Intercalation in Tungsten Disulfide

*Ruding Zhang,[#] Jingze Bao,[#] Yilong Pan, and Chuan-Fu Sun**

CAS Key Laboratory of Design and Assembly of Functional Nanostructures, and Fujian Key Laboratory of Nanomaterials

Fujian Institute of Research on the Structure of Matter, Chinese Academy of Sciences, Fuzhou, Fujian, 350002, P.R. China

[#]The authors contributed equally to this work.

*Correspondence and request for materials should be addressed to C.F.S. (cfsun@fjirsm.ac.cn)

Material and Methods

Materials. Commercial WS_2 powders (analytical pure, 99.9%) purchased from Adamas-Beta were directly used without any further treatments. Battery grade electrolytes of 1 M $LiPF_6$-ethylene carbonate (EC)-dimethyl carbonate (DMC)-10% fluoroethylene carbonate (FEC) and 1 M $NaClO_4$-EC-DMC-10% FEC were purchased from DoDoChem. Battery grade potassium bis(trifluoromethylsulfonyl) imide (KTFSI) and tetraethylene glycol dimethyl ether (DEGDME) were purchased from DoDoChem. KTFSI was vacuum dried at 100 °C for 48 hours prior to electrolyte preparation.

Materials Characterization. The phase purity and *in-situ* XRD analysis of the WS_2 material were characterized using a Rigaku Ultima IV powder X-ray diffractometer (XRD) with CuKα radiation at a voltage of 40 kV and a current of 40 mA. For *In-situ* XRD analysis, a home-made battery cell with an *X*-ray transparent Beryllium window was galvanostatic cycled using a LANHE CT2001 battery instrument at a current density of 5 mA/g, and at the same time, XRD diffraction patterns were continuously collected at a scanning rate of 6 °/min and in a 2 θ range of 5 - 65°. The microscopic and morphological features of the WS_2 powder and electrodes were analyzed on a field-emission scanning electron microscope (FESEM, HITACHI SU-8010). Transmission electron microscope (TEM, HITACHI F20) was used for the microstructure and element mapping study of the WS_2 powder and electrodes. The specific surface area was determined by Brunauer–Emmett–Teller (BET) measurement on a Micromeritics ASAP 2020 instrument. To provide a more precise evaluation, the bulk anode (including WS_2 materials, CMC binder, and carbon black) scraped directly from Al current collectors, rather than WS_2 powder, was directly used for the BET measurement.

Electrochemical Characterization. All batteries were fabricated and tested in a half-cell configuration. Electrodes were prepared through a slurry blade-coating method. Specifically, WS_2 powders were thoroughly mixed with conductivity agent (Super P carbon black, MTI Corporation) and binder (carboxymethyl cellulose, CMC, MTI Corporation) at a weight ratio of 80:10:10 with using DI water as dispersing solvent. After being stirred thoroughly overnight, the slurry was cast onto an Al foil (for Na/K-ion batteries) or Cu foil (for Li-ion batteries) by a blade-coating method. The electrode was subsequently vacuum-dried at 80 °C overnight. The mass loading of the active material (WS_2) is 2.48-2.75 mg/cm^2. CR2032-type coin cells were assembled in an argon-filled glove-box (Vigor) with both oxygen and water content lower than 0.1 ppm. A potassium metal foil was used as the counter and a reference electrode, and a glass fiber (Grade GF/F, Whatman) was used as a separator. The electrolyte was potassium bis(trifluoromethylsulfonyl) imide (KTFSI) in tetraethylene glycol dimethyl ether (DEGDME) with a concentration of 5 M. For Li/Na-ion batteries, the counter electrodes are Li and Na metal foils, respectively, with the electrolytes of 1 M $LiPF_6$-EC-DMC-10% FEC and 1 M $NaClO_4$-EC-DMC-10% FEC. The full-cell batteries were fabricated where Prussian blue $K_{1.89}Mn[Fe(CN)_6]_{0.92}$, WS_2, and 5 M KTFSI-DEGDME were used as the cathode, anode, and electrolyte, respectively. Prior to full-cell fabrication, $K_{1.89}Mn[Fe(CN)_6]_{0.92}$ and WS_2 with a mass ratio of 1.7 : 1 were separately activated for five cycles by galvanostatic cycling at a current density of 10 mA/g. The battery cyclability was tested on LANHE CT2001 battery instruments at a constant temperature of 28 °C. The voltage window was set to 0.1 - 2.0 V (versus K/K^+) for the galvanostatic test if not specified. The specific current density was set based on the mass of the active materials. When tested at a rate higher than 10 mA/g, the batteries were galvanostatically cycled once at 10 mA/g for activation before the subsequent cycling test. The specific capacities were calculated based on the weight of WS_2. The C-rates were calculated based on a maximum of 0.62 K^+ inserted into one WS_2 molecule which corresponding to a capacity of 67 mAh/g. For example, 1 C and 0.3 C correspond to 67 mA/g and 20 mA/g, respectively. Cyclic voltammetry was acquired on a Bio-Logic SP-300 electrochemical workstation with a scanning rate of 0.1 mV/s. Electrochemical impedance spectroscopy was collected by applying a sine wave with an amplitude of 10 mV over a frequency range from 100 Hz to 0.01 Hz on a Bio-Logic SP-300 electrochemical workstation. Galvanostatic intermittent titration technique (GITT) was conducted on a LANHE CT2001 instrument with current pulses of 1 hour at a rate of 10 mA/g followed by a rest step for 10 hours, and the whole process was carried out repeatedly until the cell voltage reached 0.1 V or 2.0 V (versus K/K^+). Prior to the GITT tests, all batteries were activated for one cycle by galvanostatic cycling at 10 mA/g in the voltage window of 0.1 - 2.0 V.

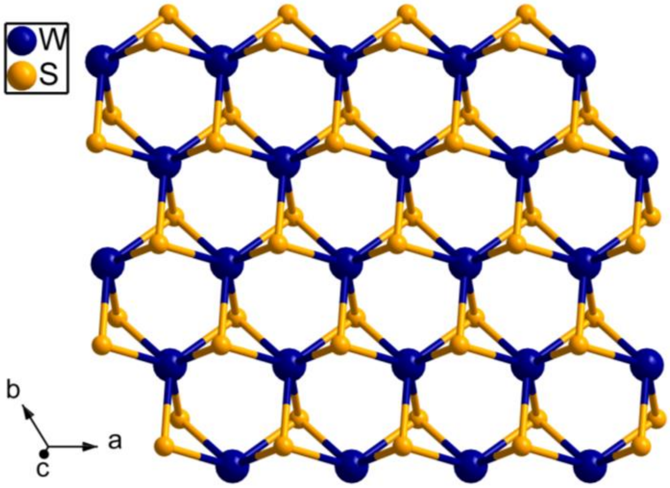

Fig. S1. View of 2H-WS_2 crystal structure along (111) direction.

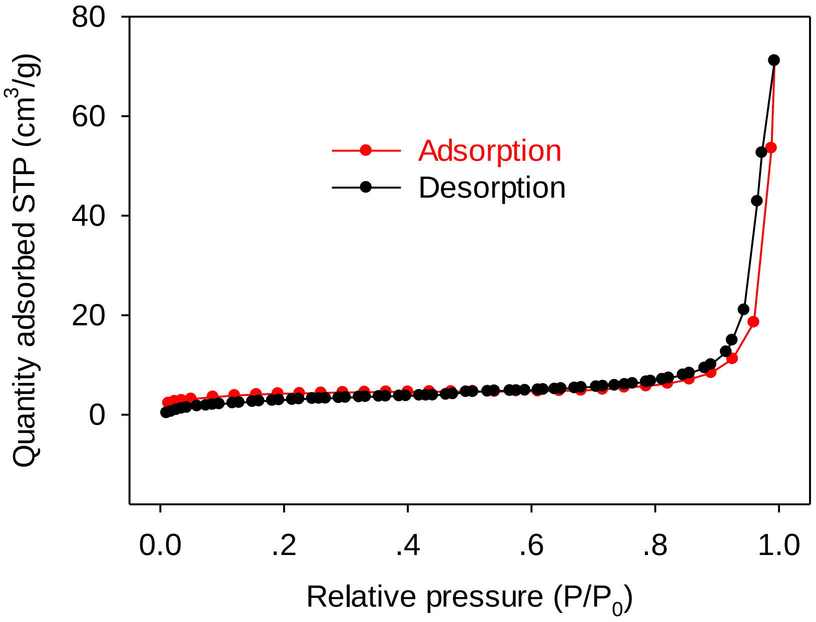

Fig. S2. Brunauer–Emmett–Teller (BET) measurement of bulk WS_2 anode together with carbon black and CMC binder (directly peeled from Al current collectors) gives a specific surface area of 14.0 m^2/g.

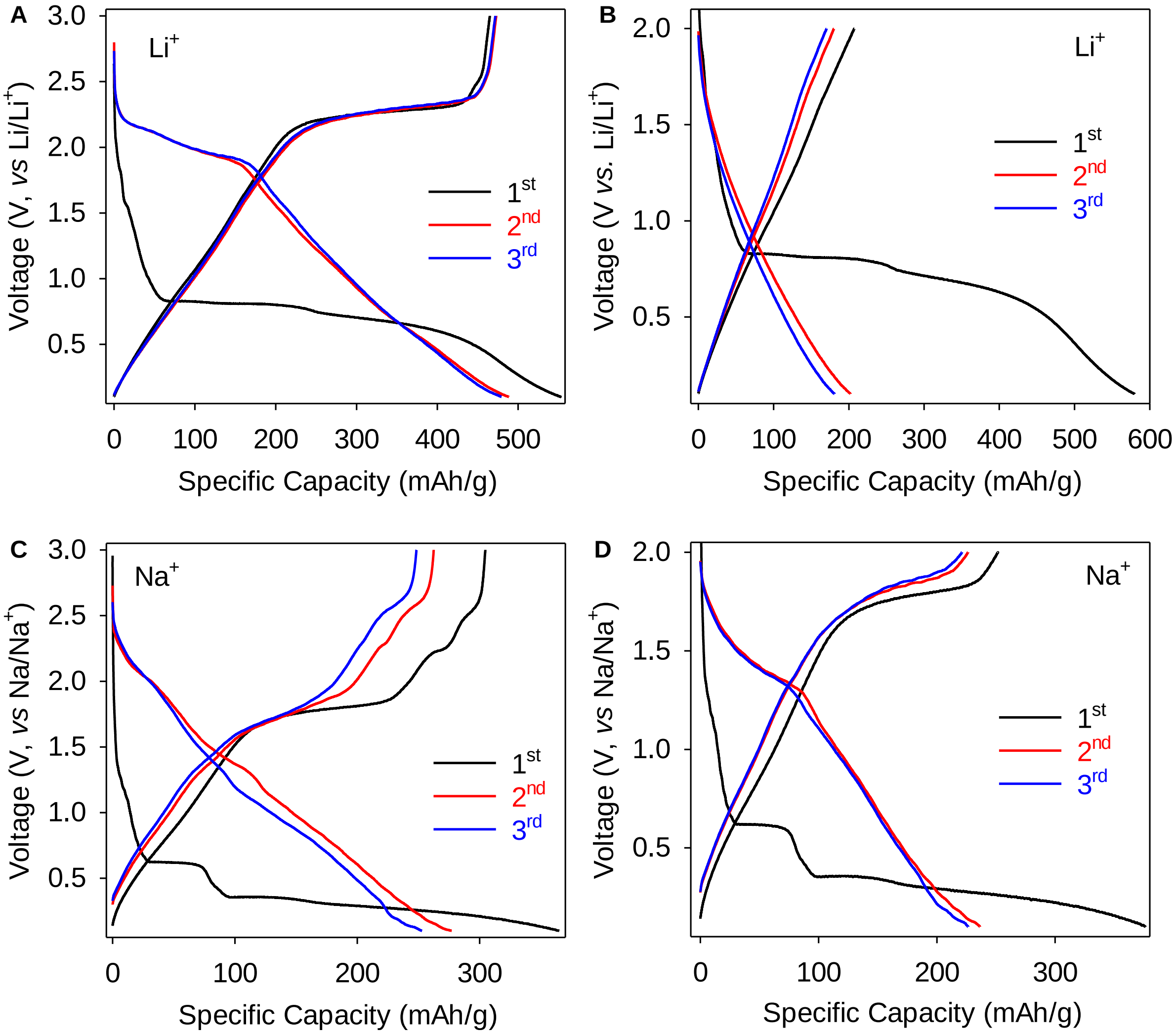

Figure S3. Electrochemical Li$^+$/Na$^+$ (de)intercalation behavior into WS$_2$. A,B, Voltage profiles of the WS$_2$ electrode in Li-ion batteries within a voltage window of 0.1-3 V (A) or 0.1-2 V (B). C,D, Voltage profiles of the WS$_2$ electrode in Na-ion batteries within a voltage window of 0.1-3 V (C) or 0.1-2 V (D). All the four batteries were cycled at a current density of 10 mA/g for the first activation cycle and a current density of 50 mA/g for the subsequent cycles.

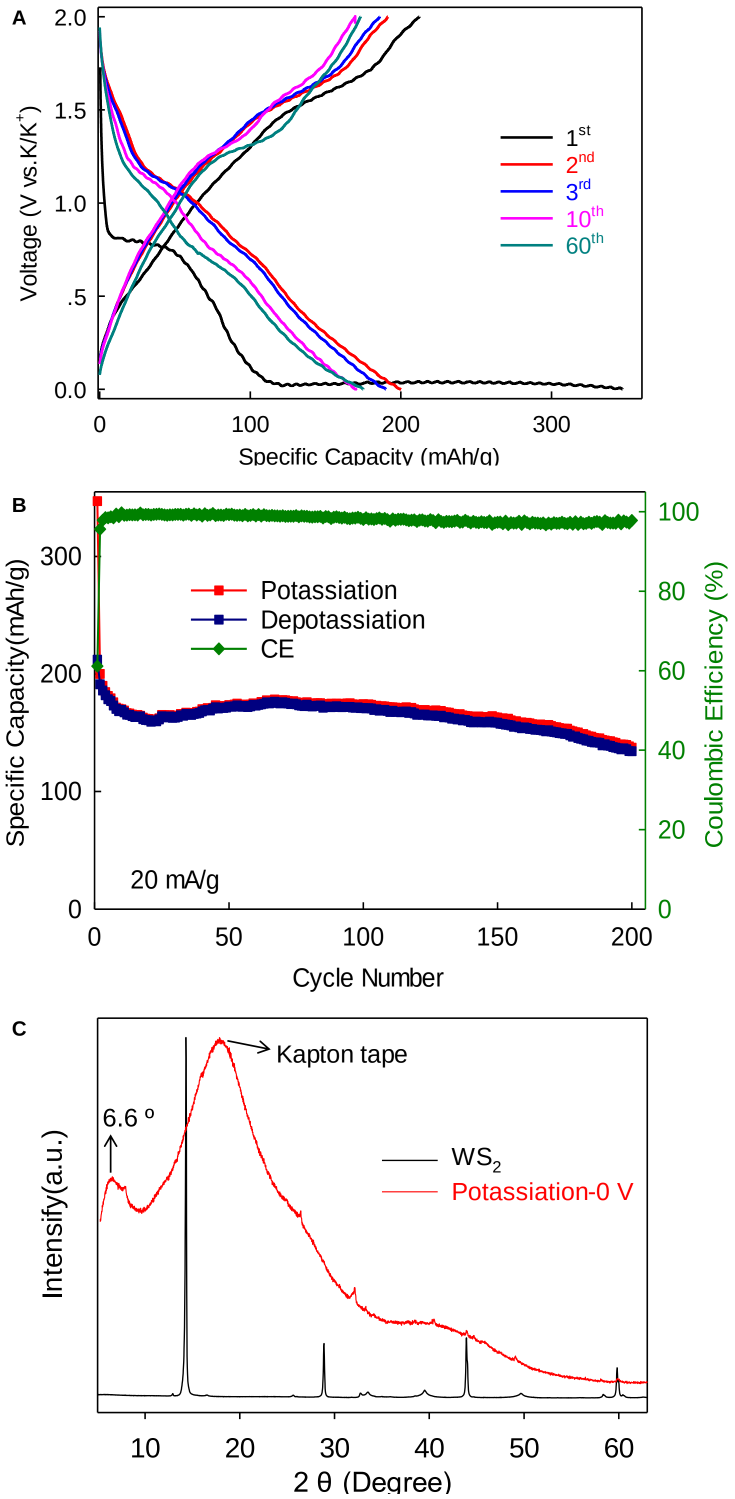

Fig. S4. Electrochemical behaviors of the WS_2 anode within the voltage window of 0 - 2 V. **A**, Voltage profiles at a rate of 20 mA/g. **B**, Cyclability and Coulombic efficiencies of WS_2 anode. **C**, XRD of initial and potassiated WS_2 anodes at 0 V (versus K/K^+).

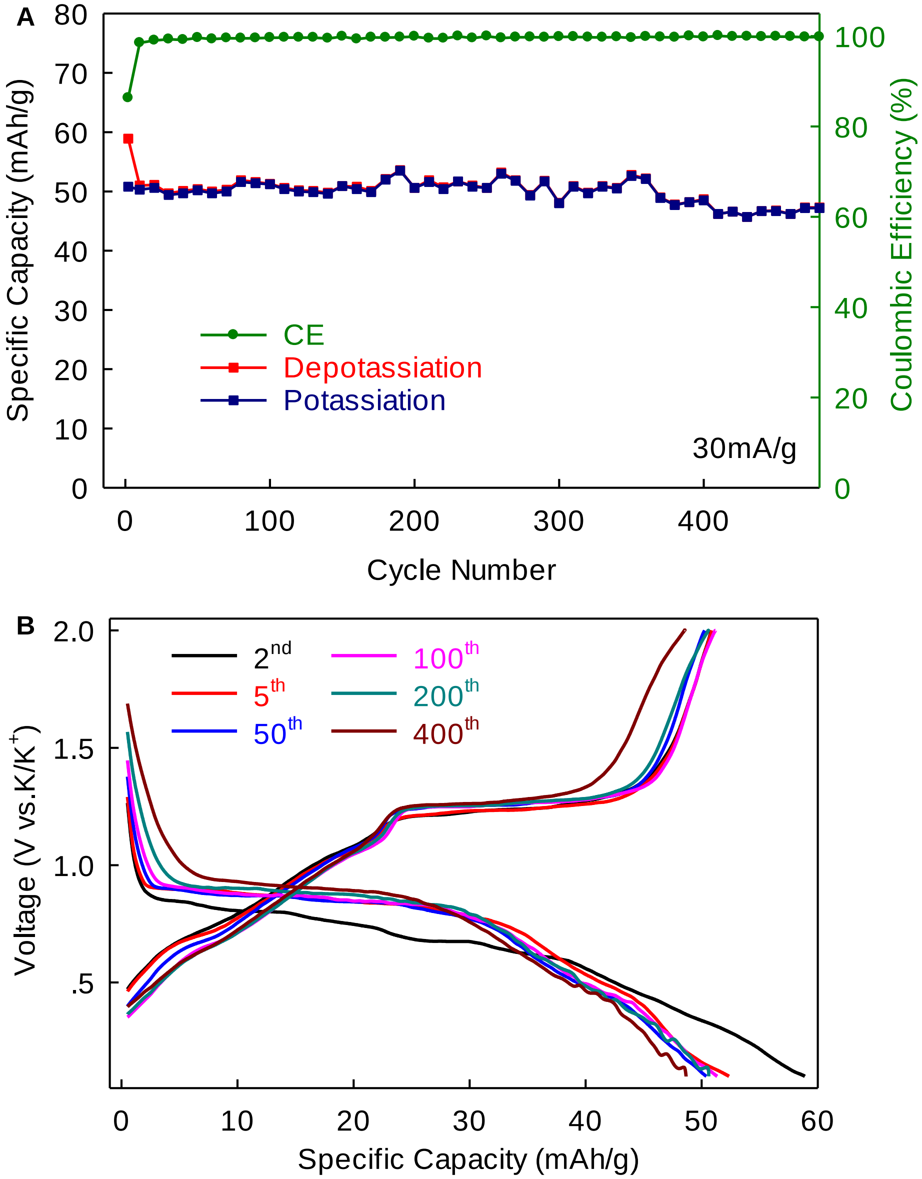

Fig. S5. Electrochemical performances of the WS_2 anode at a rate of 30 mA/g. **A**, Cyclability and Coulombic efficiencies of WS_2 anode. **B**, Corresponding voltage profiles.

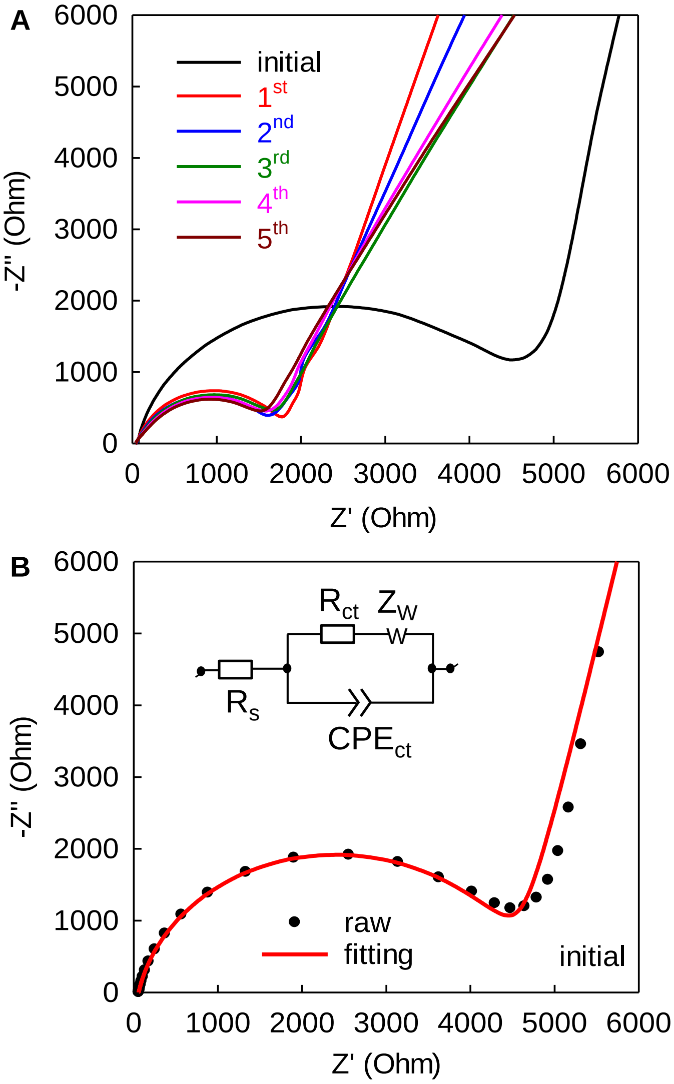

C

	initial	after 5- cycle CV
R_s (Ω)	57.73	5.46
R_f (Ω)	-	31.54
R_{ct} (Ω)	4615	1671

Fig. S6. a, EIS evolution of WS_2 anode upon CV-cycling. **b**, EIS fitting of the initial WS_2 anode. The inset shows the equivalent circuit for data fitting. **c**, Resistance derived from EIS. R_s, R_f, R_{ct}, and Z_w represent electrolyte resistance, the contact resistance of solid electrolyte interphase, charge transfer resistance, and Warburg impedance, respectively.

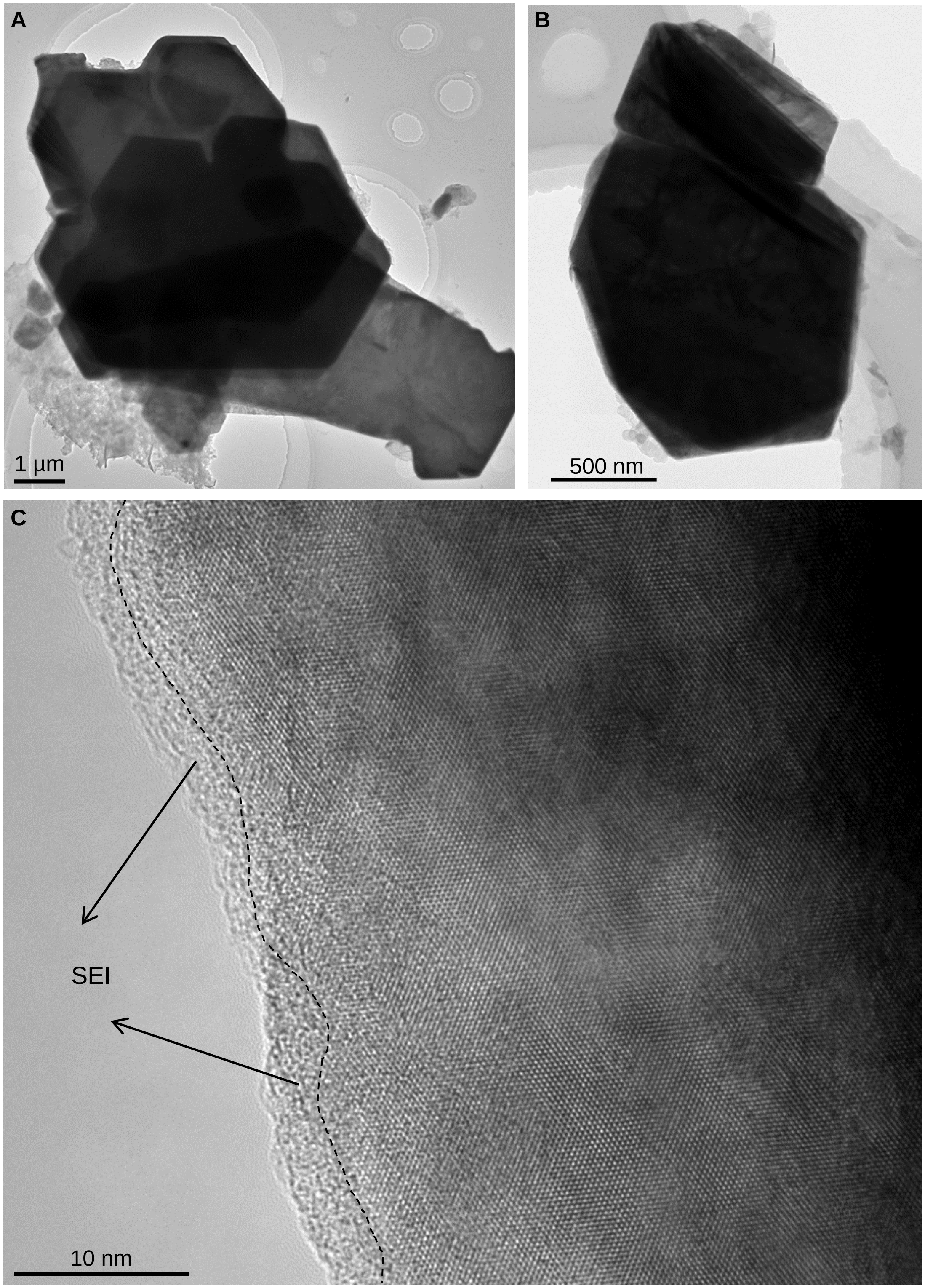

Fig. S7. TEM images of the WS_2 anode after one potassiation/depotassiation cycle.

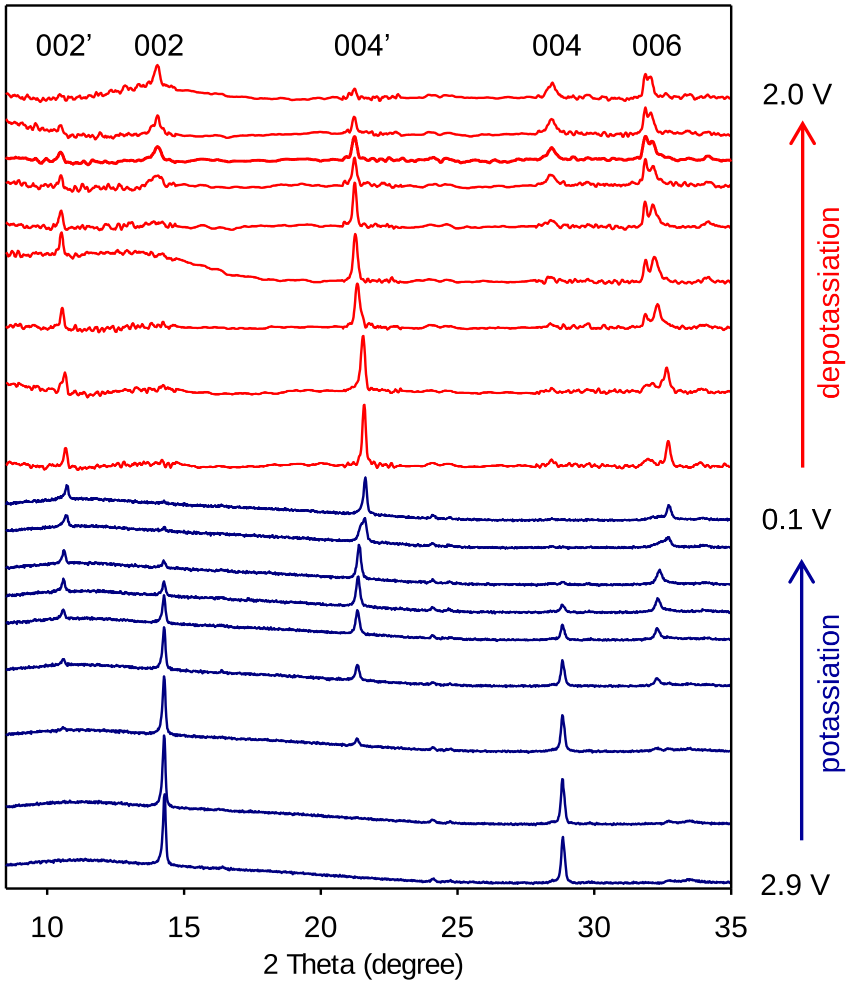

Fig. S8. *In-situ* XRD patterns collected during the first (de)potassiation cycling.

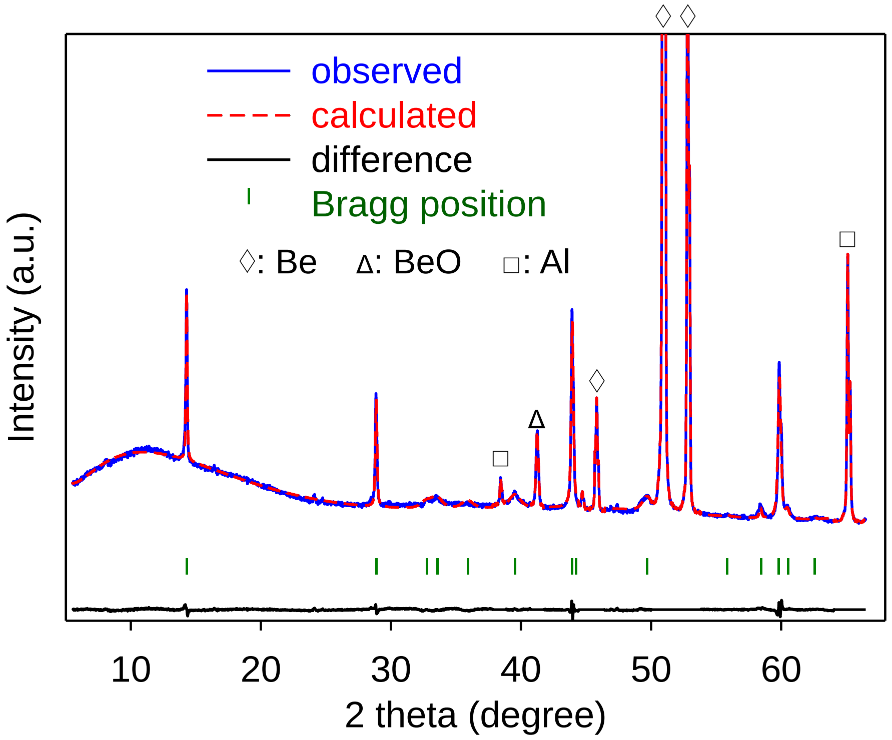

Initial WS_2: a = b = 3.156, c = 12.344, Vol = 106.478, hexagonal: P63/mmc (194), R_{wp} = 4.68%

Fig. S9. XRD pattern and the corresponding Rietveld refinement of initial WS_2 electrode.

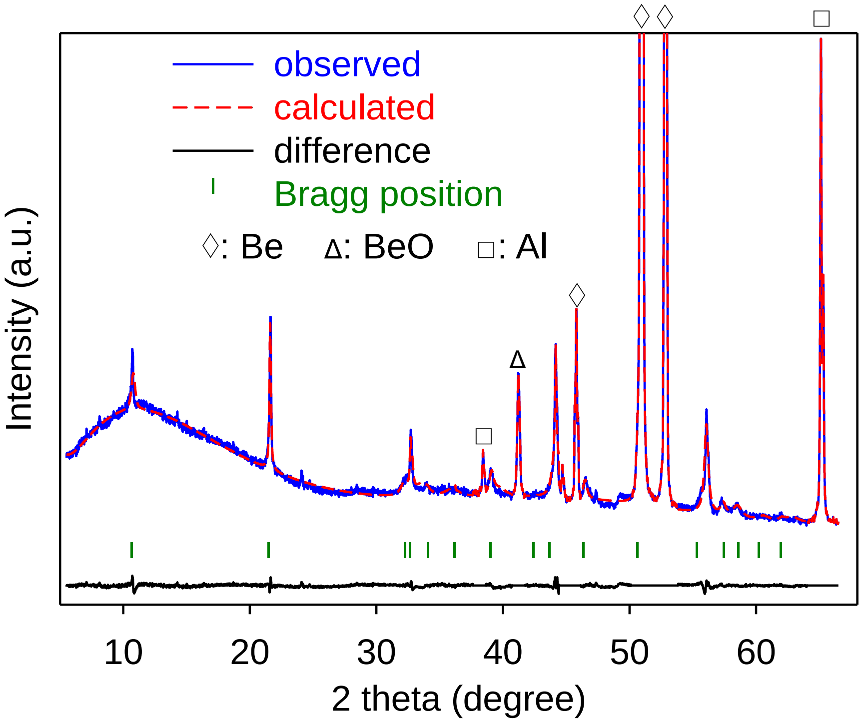

WS_2-Potassiation-0.1 V: a = b = 3.208 , c = 16.464,

Vol = 146.735, hexagonal: P-6m2 (187), R_{wp} = 4.12%

Fig. S10. XRD pattern and the corresponding Rietveld refinement of potassiated WS_2.

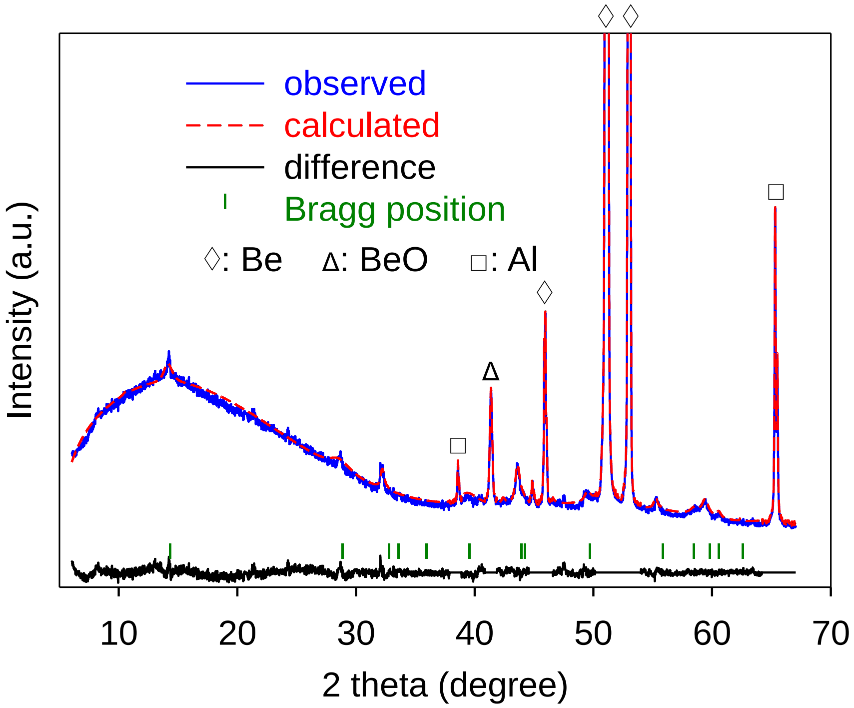

WS$_2$-Depotassiation-2.0 V: a = b = 3.147, c = 12.412,

Vol = 106.455, hexagonal: P63/mmc (194), R$_{wp}$ = 2.91%

Fig. S11. XRD pattern and the corresponding Rietveld refinement of depotassiated WS$_2$.